LOAN DOCUMENT

PHOTOGRAPH THIS SHEET

DTIC ACCESSION NUMBER

LEVEL

INVENTORY

0

Filtering Strategies for Spreading Targets

DOCUMENT IDENTIFICATION

Mar 2000

DISTRIBUTION STATEMENT A
Approved for Public Release
Distribution Unlimited

DISTRIBUTION STATEMENT

ACCESSION FOR
NTIS GRA&I ☑
DTIC TRAC ☐
UNANNOUNCED ☐
JUSTIFICATION

BY

DISTRIBUTION/

AVAILABILITY CODES

DISTRIBUTION	AVAILABILITY AND/OR SPECIAL	
A-1		

DISTRIBUTION STAMP

DATE ACCESSIONED

DATE RETURNED

20000814 198

DATE RECEIVED IN DTIC

REGISTERED OR CERTIFIED NUMBER

PHOTOGRAPH THIS SHEET AND RETURN TO DTIC-FDAC

HANDLE WITH CARE

DTIC FORM 70A JUN 90

DOCUMENT PROCESSING SHEET

PREVIOUS EDITIONS MAY BE USED UNTIL STOCK IS EXHAUSTED.

LOAN DOCUMENT

Filtering Strategies For Spiraling Targets

Paul Zarchan
The Charles Stark Draper Laboratory, Inc.
Cambridge, Massachusetts
and
Dimitrios Lianos
U.S. Army Space and Missile Command
Huntsville, AL

Abstract

Intentional or unintentional spiraling maneuvers on the part of a tactical ballistic missile target can make it particularly difficult for a pursuing missile to hit. The paper first reviews why it is difficult to hit a spiraling target with proportional navigation guidance. It is then shown that by using a special purpose linear Kalman filter that is specifically tuned for a spiral maneuver in conjunction with an advanced guidance law it is possible to dramatically improve system performance over that of a proportional navigation guidance system. However, in order for the necessary filtering and guidance to work properly the targets spiraling frequency must be known. If the spiraling frequency is unknown other methods must be used. The paper investigates two schemes for deriving the spiraling frequency of the target. The first scheme involves using a bank of Kalman filters, each of which is tuned to a different spiraling frequency. Various schemes for identifying which filter in the filter bank is tuned to the actual target frequency are investigated. The second method for deriving the target frequency involves using a single extended Kalman filter that explicitly estimates the target spiraling frequency. It is shown that such an extended Kalman filter when used in conjunction with an advanced guidance law can dramatically improve system performance.

Background

During the 1991 Gulf War hundreds of millions of TV viewers could see tactical ballistic missiles glow in the night-time skies as they decelerated through the atmosphere towards their civilian targets. In many cases TV viewers could also see the ballistic missiles spiral or corkscrew and experience complete structural failure as they appeared to explode before reaching the ground.[1,2] The purpose of this paper is to show how these phenomenon also present unique challenges for missiles attempting to intercept these highly erratic targets.

An unintentional configurational asymmetry (i.e., slight fixed fin angles resulting from manufacturing inaccuracies) will cause a tactical ballistic missile to fly with a small trim incidence known as the non-rolling trim. The presence of roll causes the tactical ballistic missile to perform a pure conical pitching and yawing motion at the roll frequency. The amplitude of the circular motion is known as the rolling trim and the motion itself is known as lunar motion. The rolling trim increases in magnitude as the rolling velocity increases. When the roll rate approximates the tactical ballistic missile natural pitch frequency it may exhibit large resonant amplification.[3,4] In other words, the resultant unintentional fin angles can cause substantial spiraling in altitude regimes which are important for endoatmospheric intercept engagements.

Miss Distance For Proportional Navigation Guidance System

An endoatmospheric interceptor guidance system consists of a seeker, noise filter and flight control system. Usually a minimum of five time constants (one for the seeker, one for the noise filter and three for the flight control system) are required to realistically express the interceptor guidance system transfer function. If accurate information on guidance system dynamics is lacking, it is often useful to choose a canonic guidance system form so that preliminary design and evaluation can take place. The binomial representation (i.e., all equal time constants) of the guidance system is the simplest possible since only one parameter, the guidance system time constant, provides all the necessary information. In the limit, as the order of the binomial transfer function approaches infinity, the guidance system will act as a pure delay. Typically the miss distances resulting from the binomial guidance system assumption will be conservative in the sense that it may yield slightly larger miss distances then will other guidance system transfer functions of the same order. The fifth-order binomial missile homing loop is shown in block diagram form in Fig. 1.

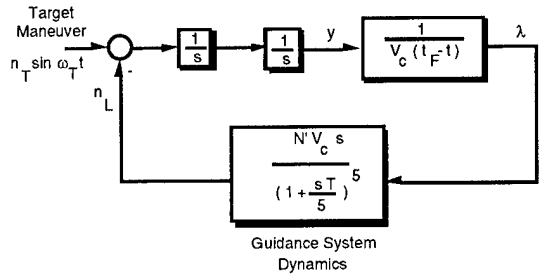

Figure 1 Fifth-order binomial guidance system

Figure 2 shows how the steady-state normalized peak miss distance due to a weave maneuver varies with the normalized target weave frequency for the fifth-order binomial guidance system.[5,6] It is interesting to note the steady-state peak miss distance is maximum when the normalized target weave frequency is approximately unity. Superimposed on Fig. 2 is the zero guidance miss distance or peak displacement n_T/ω_T^2 caused by the weaving target. Surprisingly, we can see that for the fifth-order guidance system, proportional navigation only yields a smaller miss than turning off the guidance system (i.e., N'=0) when the normalized weave frequency is less than .7 (i.e., $\omega_T T<.7$). **In other words, for normalized weave frequencies greater than .7, the weaving target nullifies the effectiveness of a proportional navigation guidance system!**

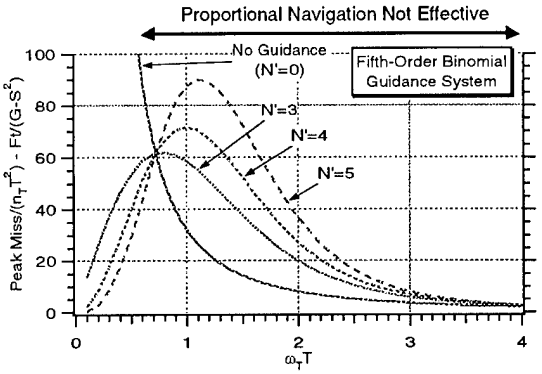

Figure 2 Steady-state peak miss due to weave maneuver for a fifth-order binomial guidance system

In order to illustrate the importance of the design curve of Fig. 2, let us consider a numerical example. Suppose we have a 6 g weaving target with spiral frequency of 1.5 r/s. Let us assume that the missile guidance system employs proportional navigation with an effective navigation ratio of 3. The time constant of the missile guidance system is .5 s. Therefore the normalized weave frequency is given by

$$\omega_T T = 1.5*.5 = .75$$

With an abscissa of .75 and for N'=3 the ordinate of the design curve of Fig.2 can be seen to be 62 or

$$\text{Peak Miss} = 62*6*.5*.5 = 93 \text{ Ft}$$

Obviously this large miss distance is not acceptable. If the weave frequency changes to 3 r/s the new normalized weave frequency is given by

$$\omega_T T = 3*.5 = 1.5$$

With an abscissa of 1.5 and for N'=3 the ordinate of the design curve of Fig.2 can be seen to be 37 or

$$\text{Peak Miss} = 37*6*.5*.5 = 56 \text{ Ft}$$

Although the new miss distance is somewhat smaller than before it is still probably unacceptable. Now that we know a spiraling target can cause large miss distances, let us see if performance can be improved by using new filtering and guidance techniques.

Linear Kalman Filter Where Weave Frequency is Known

In order to design a Kalman filter to estimate the states of a spiraling target we must first express the target maneuver in some statistical fashion. If we assume that the maneuver is sinusoidal in shape and that the starting time is uniformly distributed over the flight time we get the model of Fig. 3. In this homing system model we measure noisy relative position y* and are attempting to estimate relative position, relative velocity, target acceleration and target jerk. This model assumes that the achieved missile acceleration n_L is known. It can be shown mathematically that the shaping filter equivalent of a target maneuver with sinusoidal amplitude but random starting time (where the starting time is uniformly distributed over the flight time) is white noise through the shaping network of Fig. 3. The spectral density of this statistically equivalent white noise process is given by

$$\Phi_s = n_T^2/t_F$$

where n_T is the peak of the sinusoidal maneuver and t_F the flight time. If the ω block in Fig. 3 is eliminated from the input path, it can be shown that the preceding spectral density gets multiplied by the square of ω.

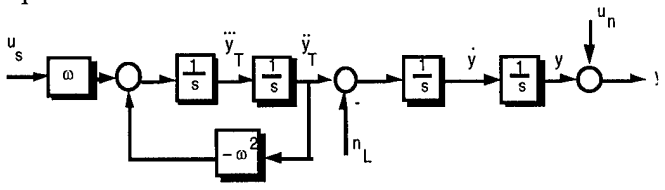

Figure 3 Homing loop model for linear Kalman filter development

We can express the model of Fig. 3 in state space

form as

$$\begin{bmatrix} \dot{y} \\ \ddot{y} \\ \dddot{y}_T \\ \cdots \\ \dddot{y}_T \end{bmatrix} = \underbrace{\begin{bmatrix} 0 & 1 & 0 & 0 \\ 0 & 0 & 1 & 0 \\ 0 & 0 & 0 & 1 \\ 0 & 0 & -\omega^2 & 0 \end{bmatrix}}_{F} \begin{bmatrix} y \\ \dot{y} \\ \ddot{y}_T \\ \dddot{y}_T \end{bmatrix} + \underbrace{\begin{bmatrix} 0 \\ -1 \\ 0 \\ 0 \end{bmatrix}}_{G} n_L + \underbrace{\begin{bmatrix} 0 \\ 0 \\ 0 \\ \omega u_s \end{bmatrix}}_{w}$$

It is important to note that the preceding equation is a linear representation of the guidance system if the target weave frequency is either known in advance or can be measured separately. Since the systems dynamics matrix **F** is time invariant the fundamental matrix Φ can be found according to

$$\Phi_k = \mathcal{L}^{-1}[\,(\,sI - F\,)^{-1}]_{t=T_s}$$

After some computation the discrete form of the fundamental matrix turns out to be

$$\Phi_k = \begin{bmatrix} 1 & T_s & \frac{1-\cos x}{\omega^2} & \frac{x-\sin x}{\omega^3} \\ 0 & 1 & \frac{\sin x}{\omega} & \frac{1-\cos x}{\omega^2} \\ 0 & 0 & \cos x & \frac{\sin x}{\omega} \\ 0 & 0 & -\omega \sin x & \cos x \end{bmatrix}$$

where

$$x = \omega T_s$$

and T_s is the sampling time (i.e., time between measurements) and ω is the frequency of the assumed weave maneuver. Again, it is important to note that the weave frequency is not estimated by this particular Kalman filter but is simply additional information required for filter operation. The measurement equation can also be expressed in discrete form as

$$y_k^* = \underbrace{[1\ 0\ 0\ 0]}_{H} \begin{bmatrix} y_k \\ \dot{y}_k \\ \ddot{y}_{T_k} \\ \dddot{y}_{T_k} \end{bmatrix} + u_k$$

where the variance of u_k, known as $\mathbf{R_k}$, is given by σ_n^2.

The four-state linear Kalman filter for the model of Fig. 3 can now be expressed in matrix form as

$$\begin{bmatrix} \hat{y}_k \\ \hat{\dot{y}}_k \\ \hat{\ddot{y}}_{T_k} \\ \hat{\dddot{y}}_{T_k} \end{bmatrix} = \begin{bmatrix} 1 & T_s & \frac{1-\cos x}{\omega^2} & \frac{x-\sin x}{\omega^3} \\ 0 & 1 & \frac{\sin x}{\omega} & \frac{1-\cos x}{\omega^2} \\ 0 & 0 & \cos x & \frac{\sin x}{\omega} \\ 0 & 0 & -\omega \sin x & \cos x \end{bmatrix} \begin{bmatrix} \hat{y}_{k-1} \\ \hat{\dot{y}}_{k-1} \\ \hat{\ddot{y}}_{T_{k-1}} \\ \hat{\dddot{y}}_{T_{k-1}} \end{bmatrix} + \begin{bmatrix} -.5T_s^2 \\ -T_s \\ 0 \\ 0 \end{bmatrix} n_{L_{k-1}}$$

$$+ \begin{bmatrix} K_1 \\ K_2 \\ K_3 \\ K_4 \end{bmatrix} \left(y_k^* - [1\ 0\ 0\ 0] \begin{bmatrix} 1 & T_s & \frac{1-\cos x}{\omega^2} & \frac{x-\sin x}{\omega^3} \\ 0 & 1 & \frac{\sin x}{\omega} & \frac{1-\cos x}{\omega^2} \\ 0 & 0 & \cos x & \frac{\sin x}{\omega} \\ 0 & 0 & -\omega \sin x & \cos x \end{bmatrix} \begin{bmatrix} \hat{y}_{k-1} \\ \hat{\dot{y}}_{k-1} \\ \hat{\ddot{y}}_{T_{k-1}} \\ \hat{\dddot{y}}_{T_{k-1}} \end{bmatrix} - [1\ 0\ 0\ 0] \begin{bmatrix} .5T_s^2 \\ -T_s \\ 0 \\ 0 \end{bmatrix} n_{L_{k-1}} \right)$$

A case was run in which there was 100 μr of range independent measurement noise on the line of sight angle. We can see from Figs. 4 and 5 that after a brief transient period the filter's estimates of the target acceleration and jerk are excellent. Of course this linear filter knows the actual weave frequency of the target.

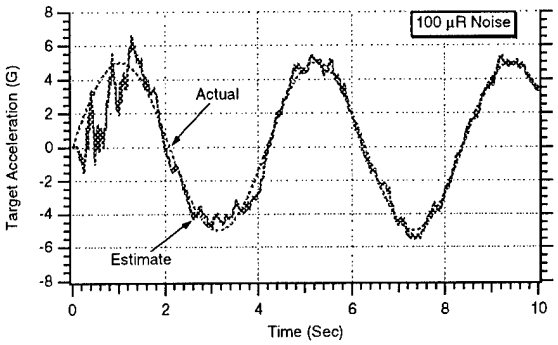

Figure 4 If frequency is known linear Kalman filter is able to track sinusoidal target acceleration

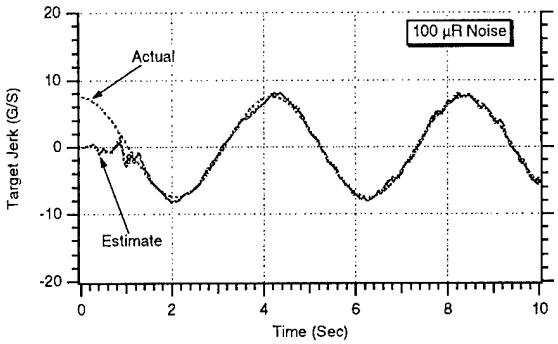

Figure 5 If frequency is known linear Kalman filter is able to track sinusoidal target jerk

Advanced Guidance Techniques

Traditional guidance laws are a form of proportional navigation PN in which the acceleration command is proportional to the measured line-of-sight rate. With this guidance law the effective navigation ratio N' is a designer chosen constant which is usually in the range of 3 to 5. Mathematically, proportional navigation can also be thought of as a guidance law in which the acceleration command is proportional to the zero effort miss and inversely proportional to the square of the time to go until intercept or[6]

$$n_c = \frac{N'}{t_{go}^2}\left(y + \dot{y} t_{go}\right) = N' V_c \dot{\lambda}$$

The zero effort miss can be thought of as a prediction of how much the missile would miss the target by if the target continued to perform as it had done in the past and the missile issued no further acceleration commands (zero effort). We can see from the preceding equation that the zero effort miss term (quantity in parenthesis) in proportional navigation assumes that the target is not maneuvering. This does not mean that proportional navigation can not hit a maneuvering target, it just means that this guidance law is not optimal in the sense that it requires the least acceleration when the target is maneuvering.

The weave guidance law, which is optimal in the sense that it requires the least acceleration against spiral maneuvers, still issues guidance commands proportional to the zero effort miss and inversely proportional to the square of time to go until intercept. However the zero effort miss is modified to account for the fact that the target is spiraling and the new guidance law can be shown to be[6,7,8,9]

$$n_c = \frac{N'}{t_{go}^2}\left[y + \dot{y} t_{go} + \frac{1 - \cos \omega t_{go}}{\omega^2}\ddot{y}_T + \frac{\omega t_{go} - \sin \omega t_{go}}{\omega^3}\dddot{y}_T \right]$$

$$= N' V_c \dot{\lambda} + \frac{N'}{t_{go}^2}\left[\frac{1 - \cos \omega t_{go}}{\omega^2}\right]\ddot{y}_T + \frac{N'}{t_{go}^2}\left[\frac{\omega t_{go} - \sin \omega t_{go}}{\omega^3}\right]\dddot{y}_T$$

where the effective navigation ratio turns out to be three. From an implementation point of view, assuming that the target weave frequency can be estimated off-line and the time to go until intercept is measured, the weave guidance law consists of three terms: one proportional to the line of sight rate, another term proportional to the target acceleration and a third term proportional to target jerk.

Figure 2 has already demonstrated that dynamics within the guidance system will cause miss distance. With endoatmospheric interceptors, the flight control system dynamics constitute the bulk of the overall guidance system time constant. If it is known that the target maneuver is sinusoidal in nature the preceding weave guidance law can be modified to compensate for the known dynamics of the interceptor flight control system. The compensated weave guidance law is very similar to weave guidance and for a single time constant guidance system can be expressed as[5]

$$n_{c_{\text{Weave-ag}}} = \frac{N'}{t_{go}^2}\left[y + \dot{y} t_{go} + \frac{1 - \cos \omega t_{go}}{\omega^2}\ddot{y}_T + \frac{\omega t_{go} - \sin \omega t_{go}}{\omega^3}\dddot{y}_T - n_L T^2 (e^{-x} + x - 1)\right]$$

where x is given by

$$x = \frac{t_{go}}{T}$$

with t_{go} being the time to go until intercept and T being defined as the approximate time constant of the flight control system. The effective navigation ratio in the compensated weave guidance law is now time-varying and is given by

$$N' = \frac{6x^2(e^{-x} - 1 + x)}{2x^3 + 3 + 6x - 6x^2 - 12xe^{-x} - 3e^{-2x}}$$

Proportional navigation and the compensated weave guidance law were evaluated for a single time constant guidance system in which the time constant of the flight control system was .3 sec. The weave maneuver had an amplitude of 5 g with a weave frequency of 1.5 r/s. The line-of-sight angle was corrupted by 100 μr of range independent noise. Figure 6 shows that proportional navigation can yield rms miss distances in excess of 15 ft while the compensated weave guidance yields rms miss distances that are near zero (i.e., hit-to-kill). Thus we can see that compensated weave guidance can dramatically reduce the miss distance when the linear Kalman filter knows the target weave frequency perfectly.

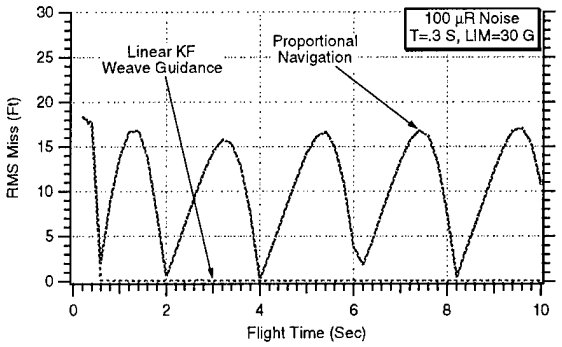

Figure 6 Performance improvements are significant with compensated weave guidance law and linear Kalman filter

Trying to Identify Weave Frequency

Since the target weave frequency is usually not known in advance experiments were conducted with the linear Kalman filter to see if information was available within the filter to determine if it was using the wrong frequency. If the filter, using self diagnosis, could identify that the frequency was wrong then a bank of filters could be used, each one tuned to a different frequency. The filter that identified itself as having the correct frequency would be the one chosen. Usually important information is available in the filter residual. In addition, we know from the Riccati equations how the filter should behave theoretically. Figure 7 displays the residual when there is only 1 μr of measurement noise and the actual target weave frequency is 2 r/s. In this case the Kalman filter weave frequency is matched to the actual weave frequency and is also 2 r/s. We can see from Fig. 7 that the single run results appear to lie within the theoretical bounds approximately 68% of the time which says theory and simulation appear to be in agreement. In addition, the single flight results indicate that the residual appears to be totally random.

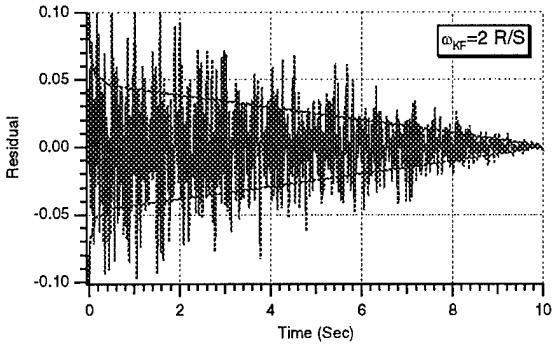

Figure 7 Residual lies within theoretical bounds when filter is matched to real world

Unfortunately, we can see from Fig. 8 that the measured residual also appears to be within the theoretical bounds when the Kalman filter estimate of the weave frequency is half of what it should be (i.e., 1 r/s rather than 2 r/s). However, we can also see from Fig. 8 that the measured residual is not as random as the residual of Fig. 7. Therefore it appears that if we are somehow able to detect that the residual is not random, we might be able to detect that the filter frequency is not matched to the real world.

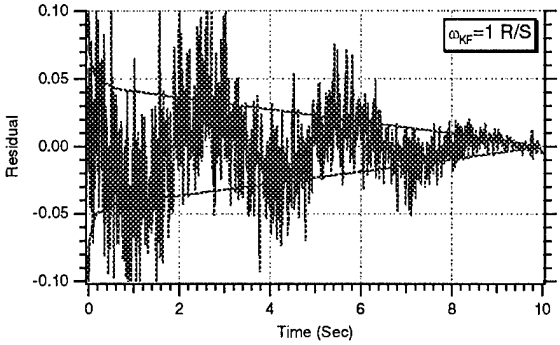

Figure 8 Amplitude of residual when filter weave frequency estimate is low does not appear to be random

Unfortunately we can see from Fig. 9 that when the Kalman filter estimate of the target weave frequency is twice what it should be (i.e., 4 r/s rather than 2 r/s) the residual not only lies within the theoretical bounds but also appears to be random. Thus, based on these "eyeball" results it appears that unfiltered residual information, by itself, does not offer sufficient information for determining if the Kalman filter weave frequency is mismatched to the real world.

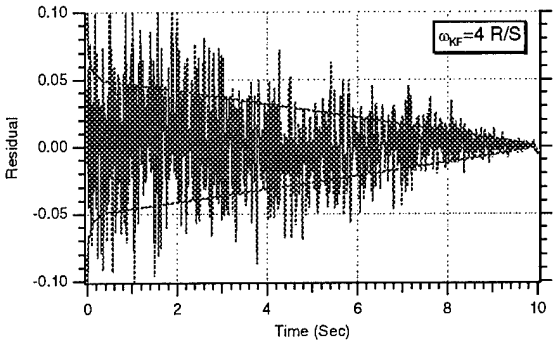

Figure 9 Amplitude of residual when weave frequency estimate is high

Filtering the Residual

A bandpass filter tuned to a frequency ω_o will attempt to pass all information at that frequency and attenuate all other frequencies. If the linear Kalman filter is matched to the target weave frequency the residual should be random which means that all frequencies are present. If we place a bandpass filter tuned to the Kalman filter weave frequency (and hence to the target weave frequency) on the residual, the resultant filtered residual should be very small. On the other hand, if the filter is mismatched to the real world, the residual will not be totally random and the bandpass filter should pass some information. This means that the filtered residual of a mismatched Kalman filter should be larger than the filtered residual of a matched filter. Figure 10 presents a conceptual block diagram for filtering the Kalman filter's residual.

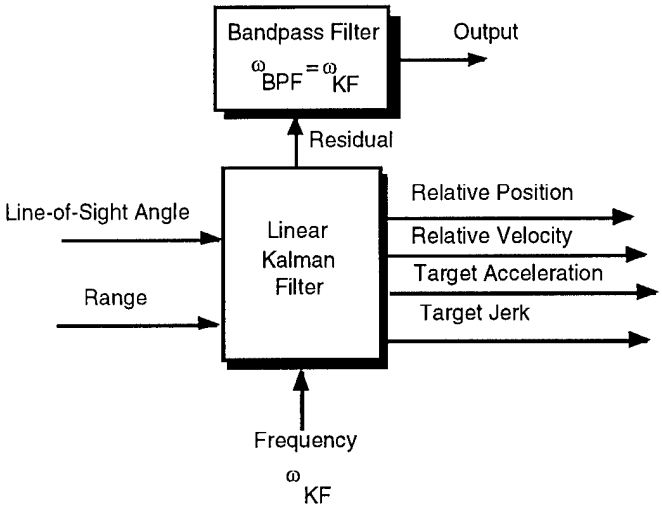

Figure 10 Filtering residual to see if filter is mismatched to real world

Cases were run with a bandpass filter on the Kalman filter's residual in which there was only 1 μr of measurement noise. We can see from Fig. 11 that when the Kalman filter and bandpass filter are both matched to the actual target weave frequency that the filtered residual is small and approaches zero after approximately 4 sec. On the other hand, we can see from Fig. 11 that when both the Kalman and bandpass filter estimates are low (i.e., 1 r/s rather than 2 r/s) the filtered residual is nearly an order of magnitude higher than it was in the matched case and does not go to zero. Instead, the filtered residual oscillates. Finally, Fig. 13, shows that when the Kalman and bandpass filter estimates are high (4 r/s rather than 2 r/s), the filtered residual is only somewhat larger than it was in the matched case (i.e., Fig. 11). However, in the unmatched case the filtered residual does not go to zero. Thus it appears that if the filtered residual goes to zero, our Kalman filter frequency must be matched to the real world. This result is important if we plan to use a bank of Kalman filters, each one tuned to a different frequency. The filtered residual which goes to zero might indicate which filter is the correct one to use.

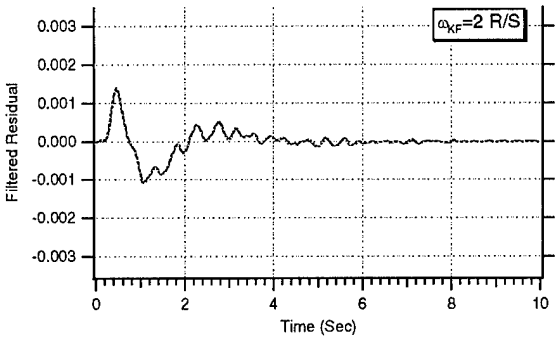

Figure 11 Filtered residual is small and approaches zero when weave frequency estimate is correct (1 μr of noise)

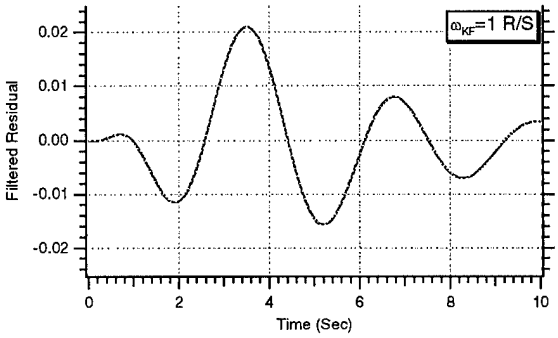

Figure 12 Filtered residual is much larger when weave frequency estimate is low and does not go to zero (1 μr of noise)

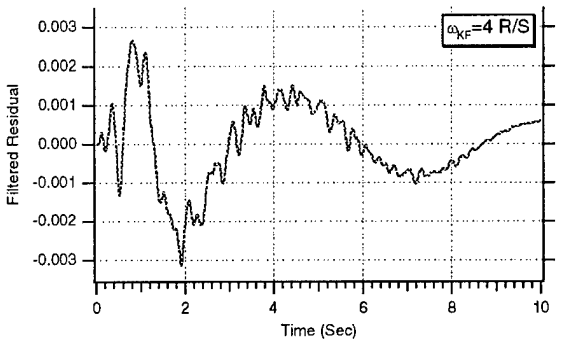

Figure 13 Filtered residual is slightly larger when weave frequency estimate is high but does not go to zero (1 μr of noise)

The previous three figures displayed filtered residual results for the case in which the there was only 1 μr of measurement noise. If the measurement noise is two orders of magnitude larger (i.e., 100 μr of measurement noise) then the results can be different. Figure 14 still shows that the residual is small (although larger than the case in which there was only 1 μr of measurement noise) and goes to zero when both filters are matched to the target weave frequency. However, it takes longer to go to zero than the 1 μr noise case (i.e., 8 sec to get to zero rather than 4 sec). In addition, Fig. 15 still shows that the filtered residual is much larger and does not go to zero when both filters frequency estimate are on the low side (i.e., 1 r/s rather than 2 r/s). However, Fig. 16 indicates that when both filter's frequency estimate is on the high side the filtered residual is only slightly larger than that of the matched case. However the filtered residual does not go to zero in this case. These results indicate that it is more difficult to use the filtered residual as an identification tool when the measurement noise is large. Thus it seems we have to explore other observables within the Kalman filter for possible identification purposes.

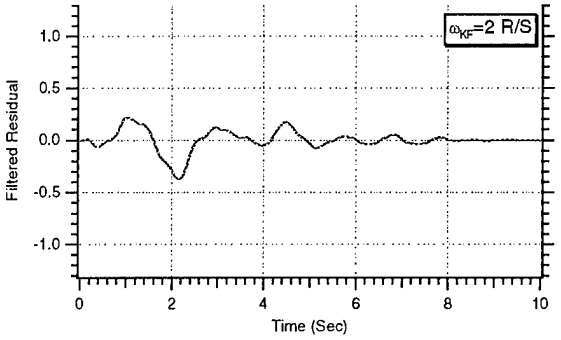

Figure 14 Filtered residual is small when weave frequency estimate is correct (100 μr of noise)

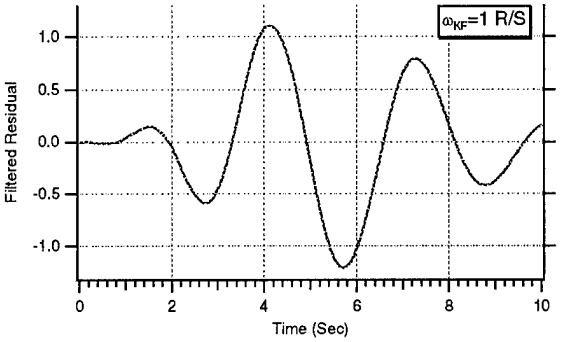

Figure 15 Filtered residual is larger when weave frequency estimate is low (100 μr of noise)

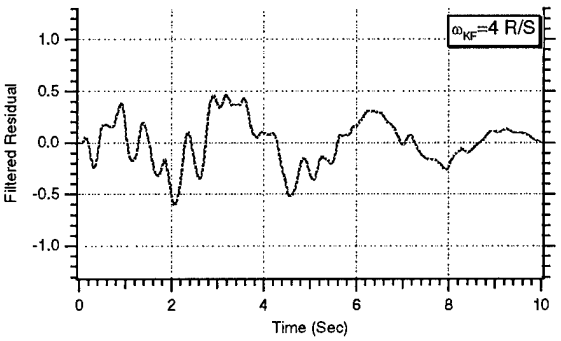

Figure 16 Filtered residual is only slightly larger when weave frequency estimate is high (100 μr of noise)

Investigating Acceleration Estimate

The Kalman filter estimates target acceleration. Although the filter will do a better job if it is tuned in frequency to the actual target acceleration, it can still estimate the frequency when the filter is mismatched. Figure 17 presents a scheme in which we will simply look at the target acceleration estimate to see if we can determine the weave frequency of the target.

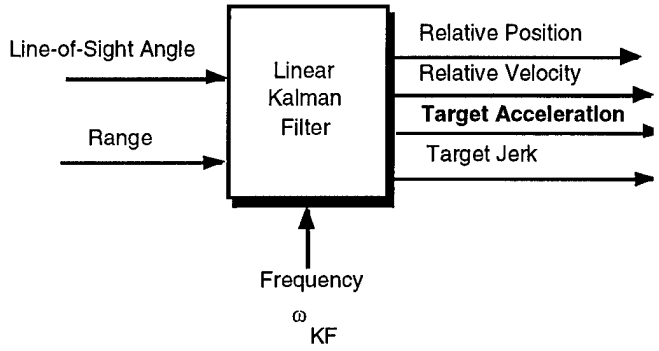

Figure 17 Is there information in acceleration estimate?

Figures 18 through 20 indicate that when the measurement noise is low all filters (i.e., matched and unmatched are able to estimate the weaving motion of the target. We can see that in all cases the period of the weaving target acceleration estimate was approximately pi which means that the target weave frequency is 2 r/s. This estimate is always correct even though the Kalman filter is sometimes not tuned correctly.

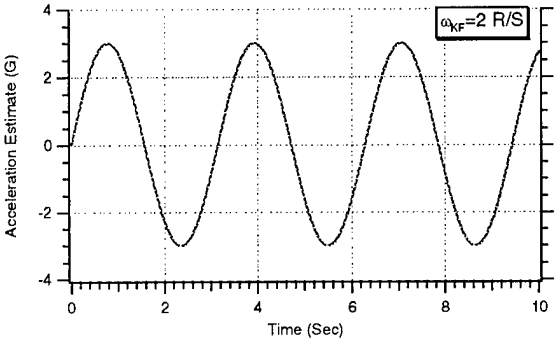

Figure 18 Filter estimates acceleration when frequency estimate is correct (1 μr of noise)

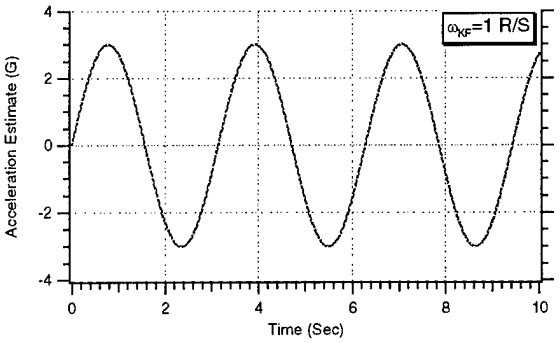

Figure 19 Filter also estimates acceleration correctly when frequency estimate is low (1 μr of noise)

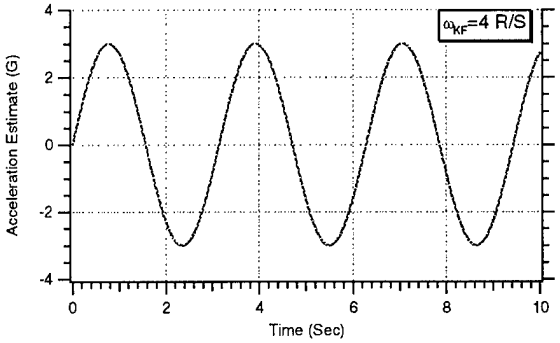

Figure 20 Filter also estimates acceleration correctly when frequency estimate is high (1 μr of noise)

If all filter frequencies yield the correct target acceleration estimate, we can then place a bandpass filter on the target acceleration estimate as shown in Fig. 21. If the bandpass filter frequency is matched to the target weave frequency than the entire estimate should be passed. However, if the bandpass filter is not tuned to the target weave frequency then the filter output will be attenuated. Thus if we have a bank of filters, the one whose filtered target acceleration estimate is largest is the one with the correct frequency estimate.

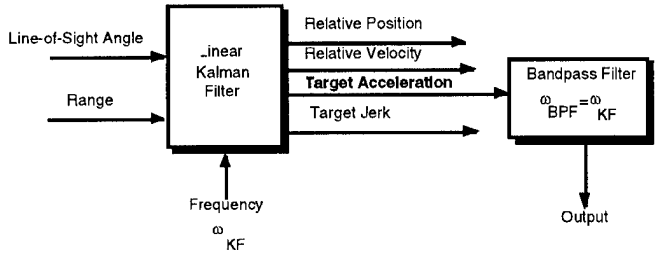

Figure 21 Does putting bandpass fillter on acceleration estimate help?

We can see from Figs. 22 through 24 that the Kalman filter whose filtered frequency estimate is matched to the actual target frequency is indeed largest. However the amplitude of the matched case is not dramatically higher than that of the unmatched case and in this case there is only 1 μr of measurement noise.

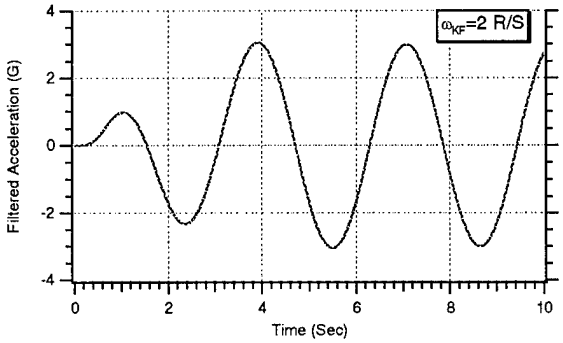

Figure 22 Filtered acceleration estimate when frequency estimate is correct (1 μr of noise)

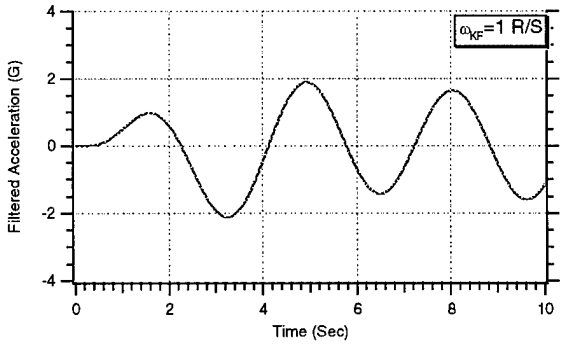

Figure 23 Filtered acceleration estimate is lower when frequency estimate is low (1 μr of noise)

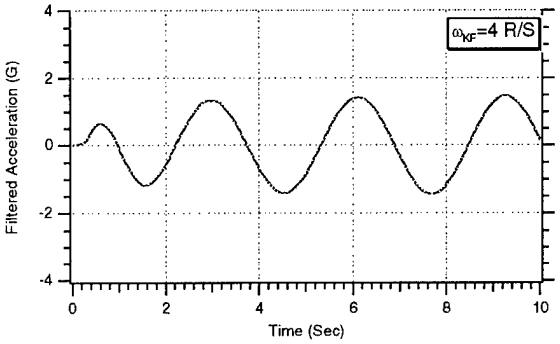

Figure 24 Filtered acceleration estimate is also lower when frequency estimate is high (1 μr of noise)

However, Figs. 25 through 27 show that when the measurement noise is increased by two orders of magnitude to 100 μr the results are not as clear. Figures 25 and 26 are near identical results which indicate that it would be very difficult with a bank of filters to determine which one was tuned to the correct frequency using the filtered frequency as an observable.

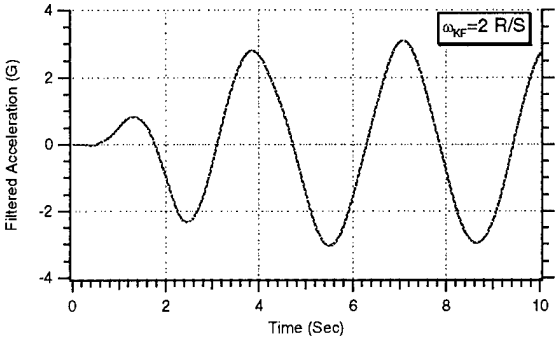

Figure 25 Filtered acceleration estimate when frequency estimate is correct (100 μr of noise)

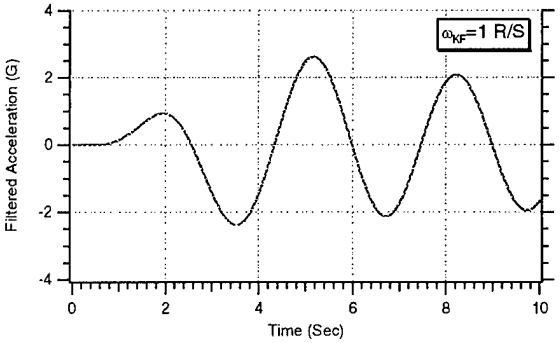

Figure 26 Filtered acceleration estimate is only slightly lower when frequency estimate is low (100 μr of noise)

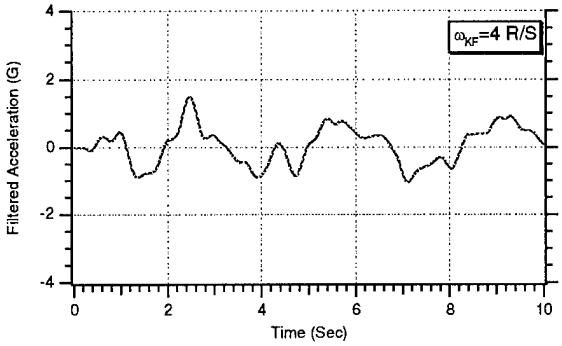

Figure 27 Filtered acceleration estimate is lower when frequency estimate is high (100 μr of noise)

Extended Kalman Filter Where Weave Frequency is Unknown

We have just seen that it is not obvious how to determine the target weave frequency by using a bank of filters. Therefore if a priori information concerning the target weave frequency is not available, another possibility is to estimate the target weave frequency. In this case, because some states are functions of the target weave frequency, the equations become nonlinear and an extended Kalman filter is required. The state equations upon which the extended Kalman filter is based are given by[10]

$$\dot{y} = \dot{y}$$

$$\ddot{y} = \ddot{y}_T - n_L$$

$$\dddot{y}_T = \dddot{y}_T$$

$$\ddddot{y}_T = -\omega^2 \ddot{y}_T$$

$$\dot{\omega} = u_s$$

The fourth differential equation of the preceding set of equations indicates that the target acceleration is sinusoidal. Since we are assuming constant target weave frequency, the derivative of the weave frequency must be zero. By setting the derivative of the weave frequency to white noise we will give the Kalman filter more bandwidth. A wider bandwidth Kalman filter will be more robust because it will be able to respond more quickly to changes in the target trajectory. From the preceding set of nonlinear state equations the systems dynamics matrix turns out to be

$$\mathbf{F} = \begin{bmatrix} \frac{\partial \dot{y}}{\partial y} & \frac{\partial \dot{y}}{\partial \dot{y}} & \frac{\partial \dot{y}}{\partial \ddot{y}_T} & \frac{\partial \dot{y}}{\partial \dddot{y}_T} & \frac{\partial \dot{y}}{\partial \omega} \\ \frac{\partial \ddot{y}}{\partial y} & \frac{\partial \ddot{y}}{\partial \dot{y}} & \frac{\partial \ddot{y}}{\partial \ddot{y}_T} & \frac{\partial \ddot{y}}{\partial \dddot{y}_T} & \frac{\partial \ddot{y}}{\partial \omega} \\ \frac{\partial \dddot{y}_T}{\partial y} & \frac{\partial \dddot{y}_T}{\partial \dot{y}} & \frac{\partial \dddot{y}_T}{\partial \ddot{y}_T} & \frac{\partial \dddot{y}_T}{\partial \dddot{y}_T} & \frac{\partial \dddot{y}_T}{\partial \omega} \\ \frac{\partial \ddddot{y}_T}{\partial y} & \frac{\partial \ddddot{y}_T}{\partial \dot{y}} & \frac{\partial \ddddot{y}_T}{\partial \ddot{y}_T} & \frac{\partial \ddddot{y}_T}{\partial \dddot{y}_T} & \frac{\partial \ddddot{y}_T}{\partial \omega} \\ \frac{\partial \dot{\omega}}{\partial y} & \frac{\partial \dot{\omega}}{\partial \dot{y}} & \frac{\partial \dot{\omega}}{\partial \ddot{y}_T} & \frac{\partial \dot{\omega}}{\partial \dddot{y}_T} & \frac{\partial \dot{\omega}}{\partial \omega} \end{bmatrix}$$

where the partial derivatives are evaluated at the current estimates. Taking the partial derivatives in this example can be done by inspection and the resultant systems dynamics matrix is given by

$$\mathbf{F} = \frac{\partial \mathbf{f}(\mathbf{x})}{\partial \mathbf{x}} = \begin{bmatrix} 0 & 1 & 0 & 0 & 0 \\ 0 & 0 & 1 & 0 & 0 \\ 0 & 0 & 0 & 1 & 0 \\ 0 & 0 & -\hat{\omega}^2 & 0 & -2\hat{\omega}\hat{y}_T \\ 0 & 0 & 0 & 0 & 0 \end{bmatrix}$$

In this example the exact fundamental matrix will be difficult, if not impossible, to find. If we assume that the elements of the systems dynamics matrix are approximately constant between sampling instants then by substituting T_S for t we can use a two term Taylor series approximation for the discrete fundamental matrix yielding

$$\Phi_k \approx \mathbf{I} + \mathbf{F}T_s = \begin{bmatrix} 1 & T_s & 0 & 0 & 0 \\ 0 & 1 & T_s & 0 & 0 \\ 0 & 0 & 1 & T_s & 0 \\ 0 & 0 & -\hat{\omega}^2 T_s & 1 & -2\hat{\omega}\hat{y}_T T_s \\ 0 & 0 & 0 & 0 & 1 \end{bmatrix}$$

The continuous process noise matrix can be found from the original state space equation to be

$$\mathbf{Q} = E(ww^T) = E\left[\begin{bmatrix} 0 \\ 0 \\ 0 \\ 0 \\ u_s \end{bmatrix}\begin{bmatrix} 0 & 0 & 0 & 0 & u_s \end{bmatrix}\right] = \begin{bmatrix} 0 & 0 & 0 & 0 & 0 \\ 0 & 0 & 0 & 0 & 0 \\ 0 & 0 & 0 & 0 & 0 \\ 0 & 0 & 0 & 0 & 0 \\ 0 & 0 & 0 & 0 & \Phi_s \end{bmatrix}$$

and the discrete process noise matrix can be found from the continuous process noise matrix according to

$$\mathbf{Q_k} = \int_0^{T_s} \Phi(\tau)\mathbf{Q}\Phi^T(\tau)\mathbf{dt}$$

In this problem we are assuming that the measurement is of the first state plus noise or

$$y_k^* = y_k + v_k$$

Therefore the measurement matrix can be obtained from the preceding equation by inspection as

$$\mathbf{H} = [\,1 \;\; 0 \;\; 0 \;\; 0 \;\; 0\,]$$

In this example the discrete measurement noise matrix is a scalar and is given by

$$\mathbf{R}_k = E(\mathbf{v}_k\mathbf{v}_k^T) = \sigma_k^2$$

We now have enough information to solve the matrix Ricatti equations for the Kalman gains.

In this example the projected states in the actual extended Kalman filtering equations do not have to use the approximation for the fundamental matrix. Instead the state projections, indicated by an over bar, can be obtained by numerically integrating the nonlinear differential equations over the sampling interval. Therefore the extended Kalman filtering equations can then be written as

$$\hat{y}_k = \bar{y}_k + K_{1_k}(y_k^* - \bar{y}_k)$$

$$\hat{\dot{y}}_k = \bar{\dot{y}}_k + K_{2_k}(y_k^* - \bar{y}_k)$$

$$\hat{\ddot{y}}_{T_k} = \bar{\ddot{y}}_{T_k} + K_{3_k}(y_k^* - \bar{y}_k)$$

$$\hat{\dddot{y}}_{T_k} = \bar{\dddot{y}}_{T_k} + K_{4_k}(y_k^* - \bar{y}_k)$$

$$\hat{\omega}_k = \hat{\omega}_{k-1} + K_{5_k}(x_k^* - \bar{x}_k)$$

The equations for the extended Kalman filter were programmed. Although the actual weave frequency in this example is 1.5 r/s, the filter's initial estimate of the frequency was misinitialized to -3 r/s to reflect the fact that the target weave frequency is really unknown. We can see from Figs. 28 and 29 that the extended Kalman filter provides excellent estimates

of the target acceleration and weave frequency when the measurement noise is 100 μr. However, by comparing Figs. 28 and 4 we can see that the extended Kalman filters estimates of target acceleration are not quite as good as the linear filter which knew the target weave frequency precisely.

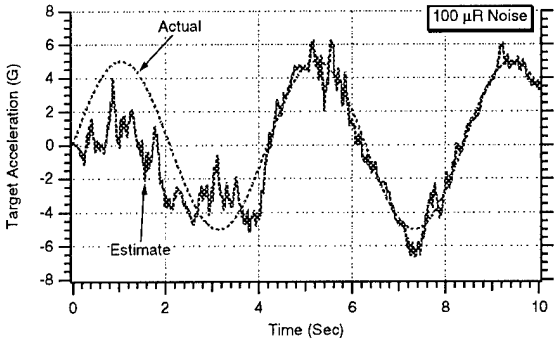

Figure 28 Extended Kalman filter is able to estimate target acceleration

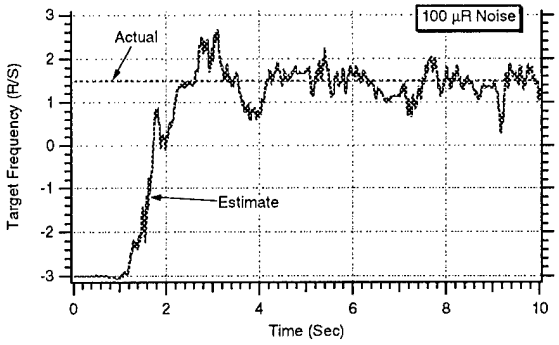

Figure 29 Extended Kalman filter is able to estimate target frequency

Miss Distance Comparison

A conceptual block diagram of the homing loop to be used for system performance evaluation appears in Fig. 30. The Kalman filter and guidance portions of the homing loop are in this figure. The two disturbances considered in the model of Fig. 7 are target maneuver and range independent measurement noise. We can see from the block diagram that a relative acceleration is formed by subtracting missile acceleration, n_L, from target acceleration. After two integrations a relative position,y, is obtained. The relative position at the end of the flight is the miss distance [i.e. Miss=$y(t_F)$]. A division of the relative position by the range from missile to target yields the geometrical line-of-sight angle λ. The line-of-sight angle is sampled every T_S seconds and contaminated by measurement noise as shown in the block diagram. The Kalman filter processes the noisy discrete angular measurements, using the achieved missile acceleration (assumed to be known perfectly), to form the required state estimates. These state estimates are processed by the guidance law to form an acceleration guidance command, n_c. In some of the experiments we will conduct the acceleration command will be limited to reflect both structural and aerodynamic constraints on the missile. In this conceptual block diagram the flight control system dynamics have been approximated by a single time constant system (i.e., first-order differential equation). The achieved missile acceleration, n_L, is the output of the flight control system and is used by both the Kalman filter and guidance law. The achieved missile acceleration also completes the feedback in the missile homing loop.

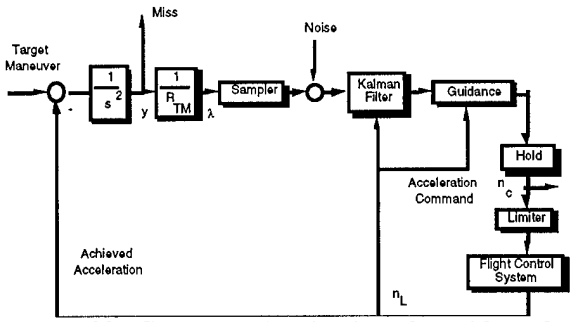

Figure 30 - Conceptual homing loop for guidance law analysis

The weave target maneuver always begins at the initiation of the flight. However, since the flight time is a parameter which varies between .2 sec and 10 sec in steps of .2 sec, we can be sure that the effect of the weaving target maneuver on each flight is different. The range independent noise, which is considered to be uncorrelated, enters the guidance system every .01 seconds (i.e., every T_S sec).

Twenty-five runs were made for each of the fifty flight times considered in order to calculate the rms miss as a function of flight time. In the experiments of this section we are comparing the rms miss distance performance of two different guidance system configurations. The first is a proportional navigation guidance system that uses a three-state linear polynomial Kalman filter to estimate relative position, velocity and target acceleration. The second guidance system configuration uses a five-state extended Kalman filter to estimate relative position, relative velocity, target acceleration, target jerk and target weave frequency.

Figure 31 shows that for the case in which there is 100 μr of measurement noise the five-state extended Kalman filter yields superior miss distance performance to that of a proportional navigation guidance system. However in the region in which the flight time is approximately 6 sec the performance of both guidance systems is approximately the same.

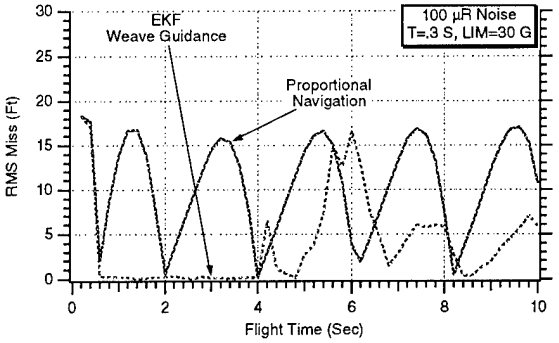

Figure 31 Extended Kalman filter yields superior performance to a proportional navigation guidance system

Figure 32 shows then when the measurement noise is reduced an order of magnitude to 10 μr the performance of the extended Kalman filter guidance system improves dramatically. We can see that now the performance of the extended Kalman filter guidance system is always superior to that of the proportional navigation guidance system. Thus we can see that the measurement noise must somehow be reduced for us to utilize the target frequency estimate in improving the guidance.

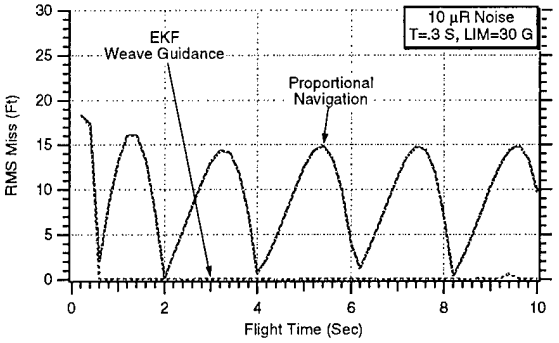

Figure 32 Performance of extended Kalman filter improves when there is less measurement noise

Summary

This paper presents different methods for improving the performance of a missile guidance system against spiraling targets. Several ad hoc schemes were explored for identifying the target weave frequency so that a linear Kalman filter and advanced guidance law could be used. None of these schemes yielded sufficiently good results when the measurement noise was large so that schemes involving banks of filters were abandoned. A more promising approach involved the use of an extended Kalman filter. The filter appeared to estimate the target weave frequency to sufficient accuracy so that there were dramatic guidance improvements. Superior miss distance performance could even be obtained when the measurement noise was large.

References

1 Riezenman, M., "Revising The Script After Patriot," *IEEE Spectrum*, Sept. 1991, pp. 49-52.

2. Canavan, G., "Strategic Defense in Past and Future Conflicts," *The Journal of Practical Applications in Space*, Vol. 2, No. 3, Spring 1991, pp. 1-42.

3 Platus, D. H., "Ballistic Reentry Vehicle Flight Dynamics," *Journal of Guidance, Control, and Dynamics*, Vol. 5, Jan.-Feb. 1982, pp. 4-16.

4 Zarchan, P., "The Challenge of Intercepting Spiraling Tactical Ballistic Missiles", *Proceedings of ION Conference*, Cambridge, MA June 1996.

5 Zarchan, P., "Proportional Navigation and Weaving Targets," *Journal of Guidance, Control, and Dynamics* , Vol. 18, Sept.-Oct. 1995, pp. 969-974.

6 Zarchan, P., *Tactical and Strategic Missile Guidance Third Edition*, AIAA Progress Series in Astronautics and Aeronautics, Vol. 176, Reston, VA, 1998.

7 Asher, R.B. and Matuszewski, J.P., "Optimal Guidance With Maneuvering Targets," *Journal of Spacecraft and Rockets*, Vol. 11, No. 3, 1974, pp. 204-206.

8 Forte, I. and Shinar, J., "Can A Mixed Guidance Strategy Improve Missile Performance," *Journal of Guidance, Control and Dynamics*, Jan.-Feb. 1988, pp. 53-59.

9 Chadwick, W.R., and Zarchan P., "Interception of Spiraling Ballistic Missiles," *Proceedings of 1995 American Control Conference*, Seattle, WA, June 1995, pp. 4476-4483.

10 Zarchan, P., "Tracking and Intercepting Spiraling Ballistic Missiles", *Proceedings of IEEE PLANS 2000 Conference*, San Diego, CA, March 2000.